A Journal of the Gesellschaft Deutscher Chemiker

D 3461

Angewandte International Edition Chemie

2004–43/1

1st January Issue

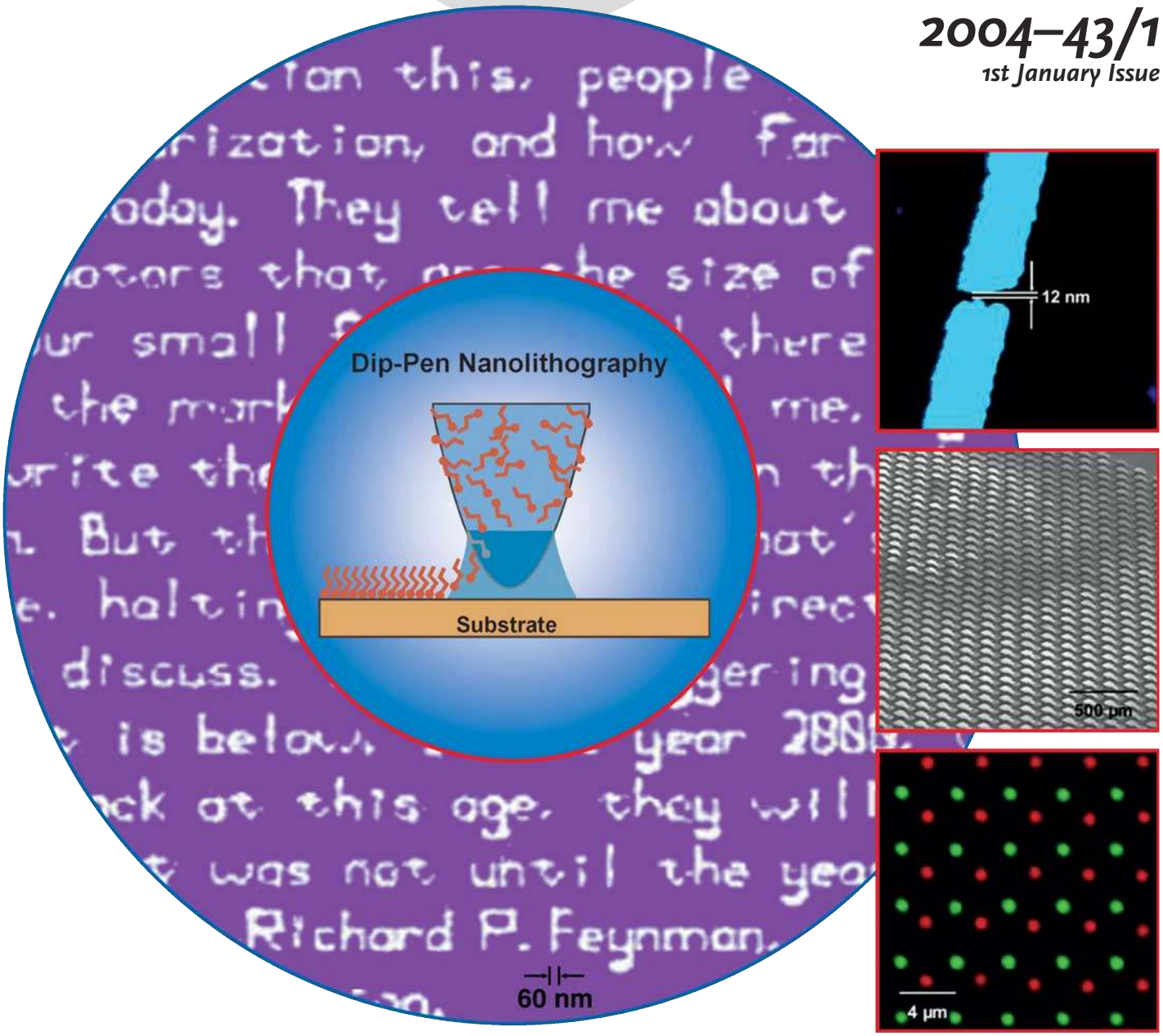

www.angewandte.org

ACIEFS 43 (1) 1–130 (2004) · ISSN 1433–7851 · Vol. 43 · No. 1 · December 22, 2003

WILEY-VCH

Nanolithography

The Evolution of Dip-Pen Nanolithography

*David S. Ginger, Hua Zhang, and Chad A. Mirkin**

Keywords:
biorecognition · dip-pen nanolithography · microarrays · nanostructures · surface chemistry

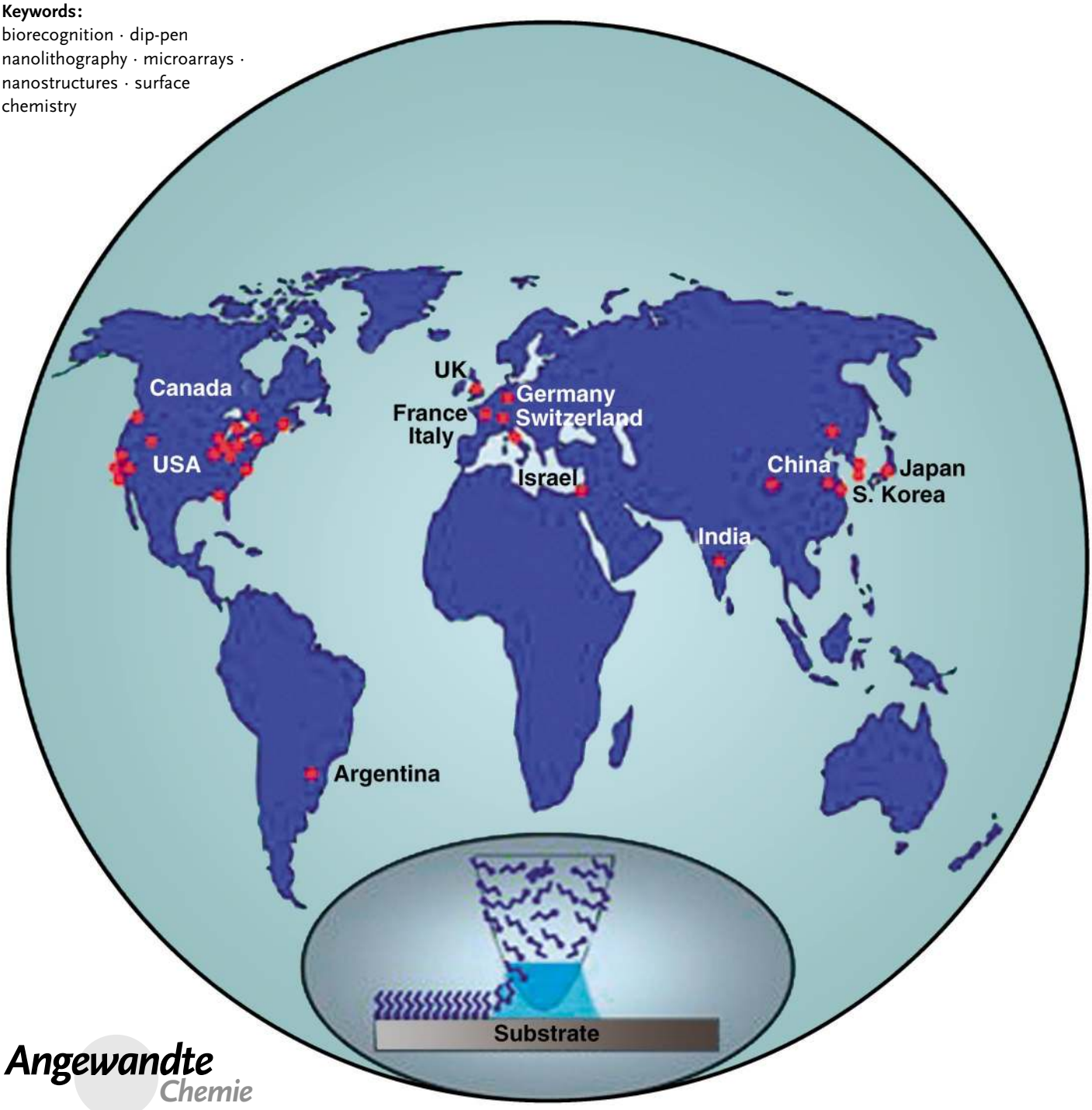

DOI: 10.1002/anie.200300608

The ability to tailor the chemical composition and structure of a surface on the 1–100 nm length scale is important to researchers studying topics ranging from electronic conduction, to catalysis, to biological recognition in nanoscale systems. Dip-pen nanolithography (DPN) is a new scanning-probe based direct-write tool for generating such surface-patterned chemical functionality on the sub-100 nm length-scale, and it is a technique that is accessible to any researcher who can use an atomic force microscope. This article introduces DPN and reviews the rapid growth of the field of DPN-related research over the past few years. Topics covered range from the development of new classes of DPN-compatible chemistry, to experimental and theoretical advances in the understanding of the processes controlling tip–substrate ink transport, to the implementation of micro-electro-mechanical system (MEMS) based strategies for parallel DPN applications.

From the Contents

1. Introduction

Developing methods that allow the chemistry of surfaces to be controlled on the 1–100 nm length scale is a fundamental and exciting challenge in nanoscience and nanotechnology because it opens new possibilities in fields ranging from molecular electronics to biomedicine to catalysis. This challenge has motivated numerous researchers since the invention of the scanning tunneling microscope (STM) and its descendents (including atomic force microscopy (AFM)). Elegant structures have been painstakingly crafted—one molecule at a time—with serial STM systems operating under ultrahigh vacuum (UHV) and at low temperatures. Other groups have used STM- and AFM-based methods to oxidize, scrape, or etch nanostructures onto surfaces. Such techniques have important applications but are generally limited to the growth of thin oxides on select metal and semiconductor surfaces, or to multistep etch-and-backfill procedures that cannot be easily generalized to the parallel patterning of multicomponent nanostructures.

In 1999 dip-pen nanolithography (DPN) was introduced to the research community as a new tool for fabricating nanostructures on surfaces.[1] DPN is a direct-write scanning-probe-based lithography in which an AFM tip is used to deliver chemical reagents directly to nanoscopic regions of a target substrate (Figure 1). Early results showed that DPN could be used to pattern alkanethiol self-assembled monolayers (SAMs) onto gold surfaces with high-resolution and registration (Figure 2 A, B).[1–3] Importantly, it was also shown that this technique offered the ability to pattern multiple chemical species with sub-100-nm alignment. It was also shown that DPN-defined SAMs were of high-quality (crystalline in the case of 1-octadecanethiol (ODT) and 16-mercaptohexadecanoic acid (MHA; thiohexadecanoic acid)) and could be used as etch resists so that both metal and semiconductor nanostructures could be generated using DPN,[4] a technique which has been refined to produce a variety of high-resolution metal and semiconductor features with controllable surface chemistry.[5,6] More

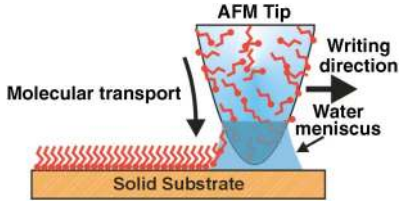

Figure 1. Schematic representation of the DPN process. A water meniscus forms between the AFM tip which is coated with "ink" molecules and the solid substrate. Reproduced with permission from ref. [1].

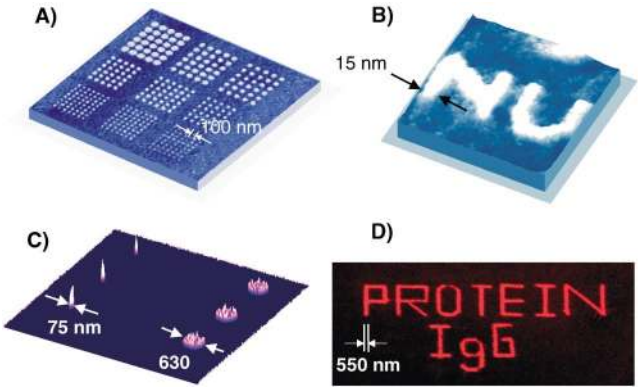

Figure 2. A) Nanoscale dot arrays written on a polycrystalline Au surface with mercaptohexadecanoic acid (MHA; thiohexadecanoic acid) by DPN[56] and B) nanoscale letters written on an Au(111) surface with MHA by DPN.[2] C) TM-AFM image of 25- and 13-nm gold nanoparticles hybridized to surface DNA templates generated with direct-write DPN (unpublished). D) Fluorescence image of direct-write DPN patterns of fluorescently labeled immunoglobulin G (IgG) on SiO_x.[46]

[*] Prof. D. S. Ginger, Dr. H. Zhang, Prof. C. A. Mirkin
Department of Chemistry
Northwestern University
2145 Sheridan Road, Evanston, IL 60208-3113 (USA)
Fax: (+1) 847-467-5123
E-mail: camirkin@chem.northwestern.edu

DOI: 10.1002/anie.200300608

Table 1: Overview of the various DPN ink–substrate combinations that have been reported.

Ink	Substrate	Notes	References
Alkylthiols (e.g. ODT and MHA)	Au	15 nm resolution with sharp tips on single crystal surfaces, <50 nm on polycrystalline surfaces	[1–7, 22, 23, 33, 87, 92, 110, 111]
Ferrocenylthiols	Au	redox active nanostructures	[59]
Silazanes	SiO_x, GaAs	patterning on oxides	[81, 111]
Proteins	Au, SiO_x	both direct write and indirect assembly	[3b, 10, 11, 30, 34, 46, 47, 67, 77, 111]
Conjugated polymers	SiO_x	polymer deposition verified spectroscopically and electrochemically	[8–10]
DNA	Au, SiO_x	sensitive to humidity and tip-silanization conditions	[12, 64]
Fluorescent dyes	SiO_x	luminescent patterns	[10, 68]
Sols	SiO_x	solid-state features	[17, 18, 112]
Metal salts	Si, Ge	electrochemical and electroless deposition	[14–16]
Colloidal particles	SiO_x	viscous solution patterned from tip	[13, 31, 65]
Alkynes	Si	C—Si bond formation	[66]
Alkoxysilanes	SiO_x	humidity control important	[109, 111]
ROMP materials	SiO_x	combinatorial polymer brush arrays	[108]

recently, DPN has been developed to pattern a variety of "ink–substrate" combinations. DPN is compatible with many inks, from small organic molecules[1–7, 109–111] to organic[8–10] and biological[11,12] polymers (Figure 2C, D), and from colloidal particles[13,31,65] to metal ions[14–16] and sols.[17,18,112] DPN can be used to pattern surfaces ranging from metals to insulators and to pattern on top of functional monolayers adsorbed on a variety of surfaces. We have even shown that DPN can be used to feed monomers to a living-polymerization reaction in a site-specific fashion, thus opening the possibility of creating and screening combinatorial arrays of polymer features.[108] An overview of the various chemistries used and the systems in which they have been applied are presented in Table 1. Many of these systems are discussed in more detail in Section 2.

As perhaps the only lithographic technique that offers high resolution and registration with direct-write printing capabilities (Figure 3), DPN is a particularly attractive tool for patterning biological and soft organic structures onto surfaces. These molecules can be deposited in either ambient or inert environments without exposing them to ionizing UV or electron-beam radiation. Furthermore, several different kinds of molecules can be deposited without exposing the substrate to harsh solvents or chemical etchants, and without risking cross-contamination—the desired chemistry is carried out exactly, and only, where it is needed.[7]

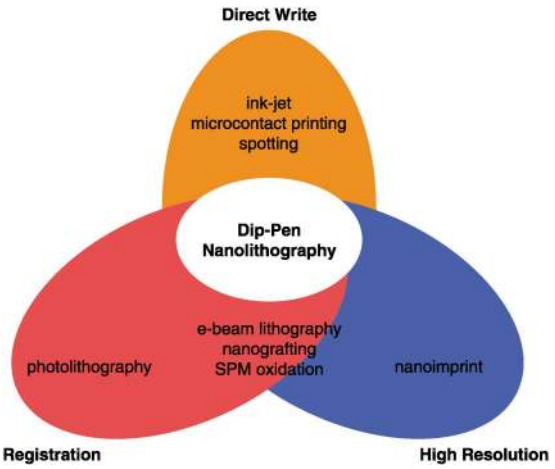

Figure 3. Comparison of the capabilities of DPN with various other lithographic tools. SPM = scanning probe microscopy.

Because of these advantages, many groups have started contributing to the development of DPN. At present, dozens of laboratories around the world have begun to study, develop, or use DPN as a tool in their own research.[8,10,11,13,15,16,19–32] The topics these workers have studied range from the fundamentals of tip-substrate ink transport,[21–23,33] to the direct deposition of metallic structures

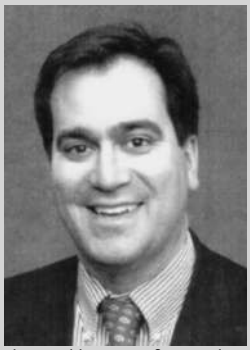

Chad A. Mirkin earned his B.S. at Dickinson College (1986) and a Ph.D. from the Pennsylvania State University (1989). After an NSF Postdoctoral Fellowship at MIT, he joined the faculty of Northwestern University where he is currently the George B. Rathmann Professor of Chemistry and Director of the Institute of Nanotechnology. He leads a multidisciplinary research program focusing on the chemistry and physics of nanoscale solution and surface architectures. His numerous awards include the Feynman Prize, the ACS Award in Pure Chemistry, the Sackler Prize from Tel Aviv University, and the Wilson Prize from Harvard University.

David S. Ginger earned dual B.S. degrees in chemistry and physics at Indiana University in 1997. He received a British Marshall Scholarship and NSF Graduate Fellowship and completed his Ph.D. in physics in the Optoelectronics Group at the University of Cambridge (UK) in 2001. He then joined Prof. Mirkin's group as an NIH Postdoctoral Fellow and a DuPont Fellow at Northwestern University. He is presently an Assistant Professor of Chemistry at the University of Washington in Seattle. His research interests center on the physical chemistry of nanoscale materials.

and development of electrochemical DPN,[8,15] to the deposition of biomolecules[12,30,34] and the effects of DPN on the organization of biopolymers.[11]

2. Applications for DPN

It is often difficult to predict the path of development that an emerging technology will follow. However, a survey of the recent literature suggests several scientific and technological areas where DPN is likely to have an important impact (although there are certainly other uses waiting for a researcher to perform the proof-of-concept and development experiments). In this section we focus on four areas in which we believe the unique capabilities of DPN are particularly likely to make an impact: patterning biomolecular micro- and nanoarrays (Section 2.1), building tailored chemical surfaces for studying and controlling biorecognition processes from the molecular to cellular level (Section 2.2), generating chemical templates for the controlled orthogonal assembly of materials on surfaces (Section 2.3), and the use of DPN as a rapid prototyping tool for generating hard nanostructures using chemical etching on a length-scale comparable, or even superior, to that obtainable with e-beam lithography (Section 2.4). The use of DPN for in situ studies of surface reactivity and exchange chemistry is discussed separately in Section 3.

2.1. Biomolecular Micro- and Nanoarrays

As a direct-write technique, DPN is particularly well-suited for patterning biological molecules on surfaces. With a resolution limit orders of magnitude better than any alternative robotic spotting or photolithographic technology, DPN has the potential to revolutionize the technology of surface-based biomolecular assays, including array-based DNA, small molecule, and protein detection. Such chip-based array-format detection systems, or "microarrays," have become ubiquitous in almost all areas of health-related research.[35–41] The power of cDNA and oligonucleotide arrays to quantify both gene expression and genomic structure (e.g. through single-nucleotide-polymorphism (SNP) detection), has led to their use in among others oncology,[38] infectious-disease pathology,[39] neurology,[40] and pharmaco-genomics,[39,41] to cite a handful of examples. Although less mature and technically more challenging than their DNA-based counterparts, protein microarrays are also under academic and industrial development.[42] In terms of array fabrication and screening technology, the resolution advantage that DPN brings to this field (Figure 4) is fundamentally exciting for two reasons: The first advantage comes from the 10000 to 100000-fold increase in areal density that could be achieved with the use of DPN. With an appropriate readout scheme, such densities would allow an assay to screen for a correspondingly larger number of targets, or, of even greater immediate impact—would allow a fixed number of targets to be screened with a correspondingly smaller sample volume, and in a shorter amount of time. In the future, one could imagine screening an entire human genome for single-nucleotide polymorphisms on a single chip using tiling methods.[36] Such an application would require a large number of conventional gene chips (over 10000 of today's state-of-the art chips (with 20-μm features)), which would require the printing and screening of an area approximately the size of a large car space in a parking lot. However, such an ambitious experiment would be feasible with a single 2×2-cm^2 chip with a spot size of 150 nm. Although major strides in bioinformatics would be required both to design as well as interpret the data from such an array, it is worth pointing out that such an application could not even be addressed with existing micron-scale technologies owing to the large chip areas and sample volumes required. The second advantage of such high-resolution patterning is that it would not only require, but also greatly facilitate, the development of high-throughput, high-resolution screening tools. While present-day detection methods may be inadequate for screening such high-density arrays, miniaturization on the scale accessible with DPN will allow the development of screening methods that are suitable for such nanoscale structures. There are many opportunities in this regard: when a feature composed of receptors is miniaturized to the scale of the biological analytes or their attached labels, almost every mechanical, electrical, and chemical property of the receptor feature is changed upon

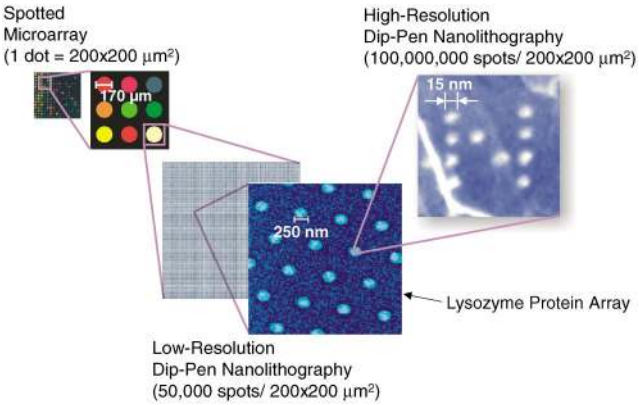

Figure 4. Schematic illustration of the power of DPN resolution in the context of biomolecular nanoarray fabrication.

Hua Zhang earned his B.S. (1992) and M.S. (1995) in chemistry at Nanjing University (China), and his Ph.D. in physical chemistry at Peking University in 1998 under the supervision of Profs. Zhongfan Liu and Xiaojie Xu. After time as a research associate using AFM to study single dendrimers in Prof. De Schryver's group in Leuven (Belgium), he joined Prof. Mirkin's group at Northwestern University as a postdoctoral fellow in 2001, where he worked on dip-pen nanolithography for fabricating solid-state metallic nanostructures by wet chemical etching. He now works at NanoInk Inc.

reaction with the analyte. These properties, which include size, shape, electrical conductivity, and hydrophilicity, all can be monitored in situ with an AFM or with on-chip electronic circuitry. In the long term, it may even be possible to direct the attachment of proteins and virus particles in specific orientations and thus to study reactivity as a function of structural configuration.

To proceed along such a path towards miniaturization will require obstacles to be overcome along the way. However, the potential rewards clearly justify the effort. One potential difficulty comes from cross-reactivity and nonspecific binding (NSB) of analyte or other species to the array spots. Although NSB is a problem for any surface-based assay, NSB is likely to become more problematic for screening on the nanoscale: on a nanoscale receptor spot it would be possible for a few nonspecifically bound particles to completely overwhelm the intended signal. Fortunately, moving to the nanoscale offers new possibilities to alleviate the NSB problem. On one hand, for a small sacrifice in information density, redundancy and "error checking" can be built into any array. On the other hand, controlling (and screening) the chemical environment with nanoscale precision could offer the opportunity both to reduce the frequency of NSB events, and to more readily identify them when they do occur. Finally, because DPN is a direct-write technology, cross-contamination of the patterned array features is entirely eliminated.

Before any of the advantages of high-resolution array patterning can be realized, it is essential to identify and develop patterning methods for particular classes of biomolecules. To demonstrate the power of DPN-based patterning and screening, we and our colleagues have used indirect adsorption techniques (Figure 5) to generate arrays of both proteins and oligonucleotides. Although it is difficult to generalize indirect techniques such as these to the fabrication of complex multicomponent arrays, single-component structures can provide powerful demonstrations as well as useful tests of array-screening performance (and can be used to investigate scientific problems in their own right, see Section 2.2). Although the patterning method depicted in Figure 5 relies on electrostatic interactions to immobilize the proteins on a surface, Zauscher, Chilkoti, and co-workers have recently demonstrated that a similar indirect approach can be used to immobilize proteins through covalent coupling.[19]

Figure 6 shows how such a DPN-fabricated protein array could potentially be used as a label-free protein-screening tool. An array of rabbit IgG protein is deposited as depicted in Figure 5. The dimensions of a single IgG molecule are $14.5 \times 8.5 \times 4$ nm, and the height of the array features after protein adsorption, (measured with AFM), are consistent with these values. Treating the array with rabbit anti-IgG leads to a 1:1 binding of the antibody–antigen IgG pairs, which results in a doubling of the average feature height, as observed in the micrographs. Perhaps more significantly, the control array (Figure 6C) which was exposed to a solution containing lysozyme, retronectin, goat/sheep anti-IgG, and human anti-IgG (without any rabbit anti-IgG) shows no change in feature height, which indicates that the patterned proteins retain their specificity. Although the orientation of

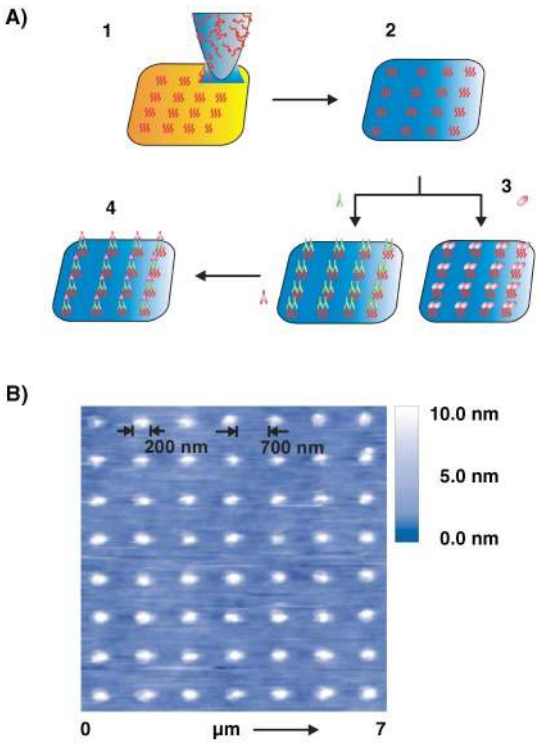

Figure 5. A) Diagram of proof-of-concept experiments, in which proteins were adsorbed on DPN-generated MHA patterns 1) MHA deposited from AFM tip onto surface, 2) passivation, 3) protein adsorption, 4) antibody recognition. The resulting protein arrays were then characterized by AFM. B) Topography image (contact mode AFM) of the retronectin protein array (reproduced with permission from ref. [34]).

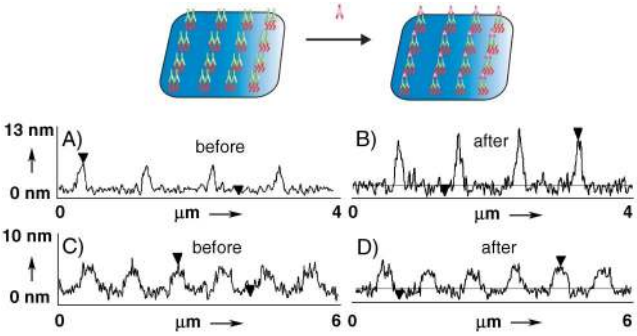

Figure 6. Height profiles of TM-AFM images: rabbit IgG assembled on an MHA dot array generated by DPN before (A) and after (B) treatment with a solution containing lysozyme, goat/sheep anti-IgG, human anti-IgG, and rabbit anti-IgG; a rabbit IgG nanoarray before (C) and after (D) exposure to a solution containing lysozyme, retronectin, goat/sheep anti-IgG, and human anti-IgG. (Portions reproduced with permission from ref. [34].)

the surface-bound IgG protein is not controlled in this experiment, a sufficient fraction of the population provides the solution-borne antibodies with access to the relevant binding domains of the protein.

Ideally, one would like to use the direct-write capabilities of DPN to fabricate biomolecular arrays with spots of many different types. Meeting this challenge requires the development of methods to coat tips reliably, the identification of

conditions for reproducible tip–substrate transport and ink–substrate coupling, and ultimately the implementation of parallel-pen and integrated-inking systems. Because the MEMs challenges of parallel-pen and integrated-inking systems are covered more fully in Section 4, this section will focus instead on the chemistry involved.

We have used direct-write DPN to pattern oligonucleotides on both metal and insulating surfaces.[12] To transfer DNA to a surface in a controlled fashion, several factors were found to be important, these include precise control of the ambient humidity and careful functionalization and inking of the AFM tips. DNA patterns could be written on gold surfaces using hexanethiol-modified oligonucleotides, and acrylamide-modified (Acrydite) oligonucleotides could be coupled with oxidized silicon wafers that had been modified with 3′-mercaptopropyltrimethoxysilane layers. The resulting patterns could be hybridized to both fluorophore-labeled oligonucleotides as well as to DNA-functionalized gold nanoparticles (Figure 7). Nanoparticle labels[43–45] are particularly promising tags for nanoscale detection applications. They exhibit a wide variety of properties—from their high molar extinction coefficients, to their physical shapes—which can be used to encode information. Indeed Figure 7B shows how a property as simple as nanoparticle size could conceivably be used as a tag in an AFM-based screening procedure, much in the way different colored fluorophores are used in optical screening. In this regard, nanoparticle labeling can serve as a bridge between the development of micro- and nanoscale detection technologies as their unique optical properties also make nanoparticles suitable for more conventional optical screening methods: Figure 7D shows an image

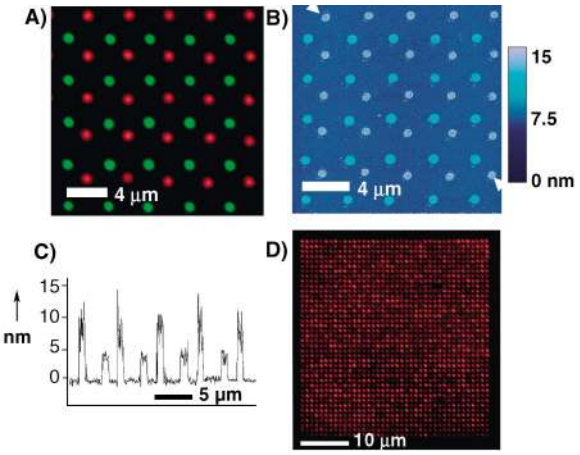

Figure 7. Direct patterning of multiple-DNA inks by DPN. A) Combined red–green fluorescence image of two different fluorophore-labeled sequences (Oregon Green 488-X and Texas Red-X) simultaneously hybridized to a two-sequence array deposited on a silanized SiO_x substrate by DPN. B) Tapping-mode AFM image of 5-nm (dark) and 13-nm (light) diameter gold nanoparticles assembled on the same pattern after dehybridization of the fluorophore-labeled DNA. C) The line plot was taken diagonally through both nanoparticle patterns, and the start and finish are indicated by the arrows in (B). D) Darkfield opitcal image showing scattering from densely packed 13-nm diameter DNA-functionalized nanoparticles hybridized to a 1600-dot DNA array patterned on SiO_x by direct-write DPN. (A–C reproduced with permission from ref. [12], D, unpublished).

of a DNA microarray with 1600 spots captured by optical microscopy.

In addition to oligonucleotides, several papers have described the formation of nanoscale protein patterns by using DPN techniques. In the first report of direct biomolecular patterning, Kaplan, Mirkin and co-workers described the deposition of thiolated collagen and collagen-like peptides onto gold surfaces using tapping-mode AFM.[11] The deposited collagen was observed to assemble into helical structures with the 65-nm periodicity that is characteristic of native collagen fiber, and fluorescence-mode near-field scanning optical microscopy (NSOM) imaging was used to confirm that the deposited structures reacted with collagen-specific antibodies. Together, these two pieces of information strongly suggest that the DPN deposition process allows, or even facilitates, the formation of native collagen structures. This result is encouraging as it provides evidence that it is possible to preserve the native/active structures of at least some types of proteins during the DPN process.

More recently, De Yoreo's group has shown that it is possible to generate nanoscale patterns of human chorionic gonadotropin antibody by direct-write DPN onto 3-glycidoxypropyltrimethoxysilane-modified glass surfaces.[10] They used proteins tagged with tetramethylrhodamine dye to facilitate imaging of the resulting patterns with confocal fluorescence microscopy. However, they did not report characterization of the biological activity of the protein patterns after deposition, so it is unknown whether the antibody retained its structure and function after the deposition and surface coupling processes. Although DPN is an extremely gentle lithographic technique, surface interactions, though apparently favorable for collagen, could potentially serve to denature other classes of proteins. Indeed, recent studies have been aimed at investigating the complex issues involved in preserving the biological activity of immunoproteins, such as IgG, during a DPN experiment and have demonstrated that it is indeed possible to deposit active immunoproteins, but that specific conditions must be maintained.[46,47]

2.2. Controlling Biorecognition Processes from the Molecular to the Cellular Level

It is fair to say that the past two years have witnessed an explosion in the types of compounds that have been patterned using DPN. Among these, biological molecules, including oligonucleotides, peptides, and proteins, have been patterned on glass and metal surfaces, generating much excitement. These advances have opened the door for research into nanoscale array-based screening technologies, as well as highlighted areas of research into DPN processes that should prove fruitful. Topics such as the preservation of protein activity and the mitigation of nonspecific binding have already been discussed in the previous section. Another important topic for future research will be improving DPN resolution. Although most of the biomolecular DPN papers published have shown high-resolution (≈ 100 nm) patterns, none have yet taken biomolecular lithography to the reso-

lution obtainable at the cutting-edge of DPN technology (currently ≈15 nm for alkanethiol inks on single-crystal gold surfaces).[2] Such sizes are commensurate with the size of individual biological macromolecules, which offers the tantalizing possibility that DPN could be used to position individual structures with molecular resolution to create tailored chemical surfaces that would allow the investigation of a variety of biological recognition processes spanning the molecular to the cellular level. The development of even higher-resolution DPN techniques may require the use of high aspect ratio AFM tips (such as carbon nanotubes[48]) or the combination of DPN with techniques such as nanografting. The DPN–nanografting combination was described by G.-y. Liu and co-workers in a method they call the "nanopen-reader-writer" (NPRW) (Figure 8).[20,49] NPRW employs a

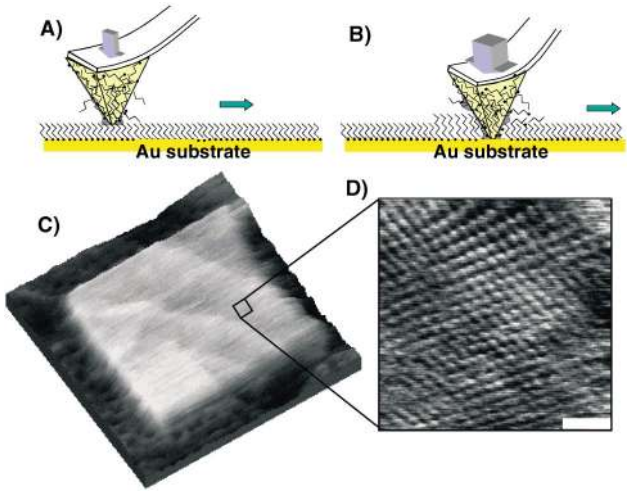

Figure 8. DPN can be combined with other scanning-probe lithography techniques, such as nanografting, to retain the advantages of each. A) In the "nanopen-reader–writer" (NPRW) system, the surface is first passivated with a bulk self-assembled monolayer. B) By applying a high contact force the tip shaves away some of the passivating molecules, which allows the ink from the tip to generate patterns in direct-write fashion. C) A 200×200 nm^2 square with sharp corners prepared using NPRW by depositing C_{18} thiol in a C_{10} monolayer. D) A high-resolution topograph of the patterned region, scale bar is 2 nm. Images courtesy of G.-y. Liu.

bulk SAM passivation layer to inhibit writing except under conditions of high applied contact force, thus decreasing the sensitivity of DPN to ambient conditions and ink-diffusion rates while bringing the direct-write and ambient-compatibility of DPN to the nanografting community. Electrochemical modification of SAM patterns provides another route towards feature-size reduction.[50] By controlling the electrochemical potential of a patterned substrate, it is possible to selectively address different regions of a pattern with distinct desorption potentials. Because thiols at the edge of a surface feature are less stable than those in its center, DPN patterned structures can be shrunk in an electrochemical "whittling" process that allows the feature sizes of an entire array of patterns to be reduced in parallel (Figure 9).[50]

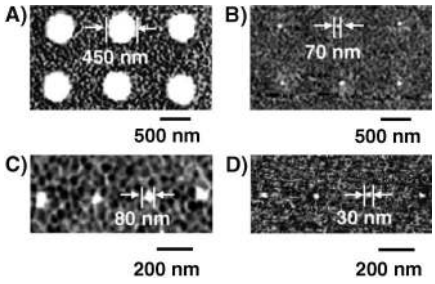

Figure 9. Electrochemical "whittling" of DPN patterns. Lateral force microscopy (LFM) images of MHA patterns before and after electrochemical desorption. A) and C) an MHA dot pattern. B) The pattern in (A) after 6 min desorption at −750 mV (Ag/AgCl reference electrode). D) The pattern in (C) after 1 min desorption at −750 mV (Ag/AgCl reference electrode). (Reproduced with permision from ref. [50].)

Even without special modifications, the length scales accessible to DPN have already opened new possibilities in studying cellular adhesion processes. Many types of cells have evolved a complex system of ligand–receptor interactions through which they recognize and interact with their external environment.[51] The ability to pattern these ligands on surfaces on the micron, nanometer, and potentially even molecular scale, is allowing the investigation of cell–receptor interactions in entirely new experiments. To demonstrate the potential of this method, our group and the Mrksich group fabricated nanoarrays of retronectin (a recombinant cellular adhesion protein based on fibronectin) using DPN.[34] Cells adhere to retronectin through the binding of integrin receptors.[51] As a cell adheres to and spreads across a surface, the integrin receptors associate into clusters comprising several other proteins to form a focal adhesion complex. Previously, lithographic methods capable of varying the size and spacing of retronectin features on surfaces had been limited to micron-scale resolution, which makes them incapable of probing the typical distribution of focal adhesion sizes (50–500 nm).[51] Using DPN, it was possible to pattern 200 nm Rectronectin features and demonstrate that cells were able to adhere to and to spread on the DPN patterns (though not as much as on unpatterned retronectin-coated surfaces). Because the sizes of the focal adhesion complexes are believed to be 50–500 nm, DPN provides a particularly powerful tool to study the distribution of focal adhesion sizes, and the effects of retronectin domain size and spacing on cellular adhesion. With direct-write DPN, it should even be possible to study interactions between cells and surfaces patterned with multiple ligands on multiple length-scales. Such an experiment would be extremely difficult if not impossible to perform with conventional lithographic or stamping processes, which are inherently indirect or single-ink processes.

As the methods for depositing both small organic molecules and large biomolecules using DPN are refined, additional opportunities for tailoring surface-bound ligand–receptor interactions will certainly present themselves. Eventually, it may even be possible to control the attachment of individual entities—such as large proteins or viruses—to surfaces in specific locations, and with well-controlled ori-

entations. As a step towards this goal, the immobilization of both native and genetically engineered cow pea mosaic virus (CPMV) particles on DPN patterns has been studied.[52,53] In that work, CPMV particles were used which had been engineered to express cysteine groups at the vertices of the icosohedral virus capsid.[54,55] These particles can be selectively immobilized onto bifunctional linkers that have been patterned via DPN.[54,55] De Yoreo and co-workers demonstrated that molecules with a thiol on one end, and an amine on the other, could be patterned at very high ($\approx$50 nm) resolution (Figure 10).[53] A heterobifunctional linker can then be used to couple the exposed amine groups on the pattern with the exposed cysteine groups on the engineered CPMV.[53]

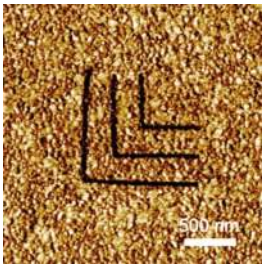

Figure 10. Fifty-nanometer wide lines of a bifunctional amine-thiol linker molecule deposited on gold by DPN. The patterns were used to mediate the adhesion of virus particles to the surface. Reproduced with permission from ref. [53].

Smith et al. also demonstrated that DPN could be used to deposit mixed monolayers to finely tune CPMV immobilization.[52] Although monolayers of 100% maleimide will covalently bind engineered CPMV particles, under certain conditions they can also nonspecifically adsorb non-engineered wild type CPMV (as well as a large number of proteins) owing to hydrophobic interactions. Thus, the selective immobilization of specifically engineered virus particles on DPN-generated patterns is aided by the deposition of mixed monolayers from coated AFM tips. With improvements in the resolution of DPN, or through the use of larger virus particles, it should be possible to control the distribution of particles on the surface and even to immobilize individual particles in specific locations. A number of proteins and viruses possess characteristic dimensions which are tantalizingly close to the resolutions obtainable with DPN, and it is anticipated that controlling the attachment and orientation of such particles on surfaces for studies of biorecognition processes on a variety of length scales will provide a fruitful area of study.

2.3. Building Nanostructured Materials with DPN: Templates for Orthogonal Assembly

Outside of biology, the surface-templated assembly of particles with sub-micrometer to sub-100-nanometer dimensions is of interest to researchers working in fields ranging from colloidal crystallization to magnetic information storage, and from photonics to nanoscale electronics. As DPN offers a rapid method of structuring the surface chemistry of a variety of substrates on these length-scales, it can provide a powerful approach to investigating problems in these fields.

We have developed a number of DPN-based methods for controlling the immobilization of particles with diameters ranging from 5 nm to nearly 1 μm onto surfaces. Electrostatic interactions between MHA and amine- or amidine-coated polystyrene spheres can control the immobilization of 190 nm to 930 nm diameter particles with single-particle precision.[56] Although others have used techniques ranging from microcontact printing to optical tweezers to position similarly sized particles on surfaces,[57,58] the flexibility and relatively high throughput of DPN allowed templates to be screened for particle adsorption in a combinatorial fashion. By preparing a large number of test templates on a single substrate, DPN could be used to quickly identify the optimal conditions for immobilizing single particles in a single experiment.[56] Furthermore, we have shown that electrostatic particle assembly can be used to form arrays of magnetic nanostructures.[110]

One limitation of electrostatically directed particle assembly is the binary nature of the interaction pairs—surfaces can be programmed only with positive or negative charges, thereby limiting the information content of a particular pattern and the complexity of the particle-based structures which can be assembled with such a technique. To increase the complexity of structures that can be generated with electrostatic DPN templates, we turned our attention to redox-active ferrocenylalkylthiol inks.[59] By choosing inks with differing redox potentials, the oxidation state and surface charge of the patterned molecules can be tailored by controlling the electrochemical potential of the substrate. This approach allows finer control over electrostatically directed particle assembly, thus allowing the orthogonal assembly of different sizes of nanoparticles.

In terms of information content, biological molecules offer the potential to encode vastly more information than synthetic chemical systems. Indeed, billions of years of evolution have resulted in a highly efficient biochemical information-storage system based on nucleic acids, and we and others have studied the use of DNA to direct the assembly of a variety of nanoparticle-based systems over the past few years.[60–63] The potential to imprint a surface with a virtually limitless quantity of information (a 15-mer of DNA offers 4^{15} different possibilities, and working with longer sequences extends this range even further) and the possibility of doing so with the exceptional resolution of DPN has motivated the development of DPN-based DNA patterning techniques. The first approach used to control the orthogonal assembly of nanoparticles relied on the indirect patterning of DNA: MHA was patterned using DPN, and then carbodiimide chemistry was used to link amine-functionalized oligonucleotides to the surface.[64] While multiple sequences can be deposited using indirect methods, each additional sequence requires its own additional patterning and coupling steps, which can ultimately lead to cross-contamination of the patterns, which highlights the disadvantage of indirect lithographic processes. It was for these reasons that direct-write

DPN strategies were developed for depositing DNA onto surfaces using chemically modified AFM tips and precisely controlled environmental conditions (Section 2.1).[12] Using such a strategy, sequence-specific interactions can be used to direct the assembly of DNA-functionalized particles into a number of predefined nanopatterns (see Figure 7). In some respects, DNA is the ideal molecule for DPN-based template generation: although considerable effort was required to prepare cantilevers and identify conditions amenable to direct-write DNA patterning, the virtually limitless range of DNA sequences available means that an enormous number of ligand–receptor pairs can now be patterned using nearly identical experimental conditions.

Although the focus of this Review has so far been on generating templates for particle assembly, it is also possible to use DPN to directly place nanoparticles, or generate solid nanostructures, in specific locations on surfaces. For instance, Brust, Ondarcuhu, and co-workers inked an AFM tip with a concentrated liquid solution of alkanethiol-capped gold colloid.[13] By controlling the contact force they were then able to deposit 5 nm diameter particles in clusters of 50–200 nm in diameter depending on the contact force used,[13] and a similar method was recently reported by G.-y. Liu and co-workers.[65]

In another direct-patterning approach for hard-nanostructure fabrication, J. Liu and co-workers have used both electrochemical and electroless versions of DPN to deposit metal nanostructures on surfaces.[14,15] By using the water meniscus not only as a transport medium, but also as a nanoscale electrochemical cell, they were able to deposit Pt, Au, Ge, Ag, Cu, and Pd through electrochemical reduction onto a Si surface in a technique they termed E-DPN (electrochemical-DPN).[14] Significantly, they also showed that the deposited features were not the result of anodic oxidation of the Si, but rather arose from metal reduction. Later, they were able to demonstrate that metals could also be deposited without an applied bias. In that work DPN was used to deliver $HAuCl_4$ to an HF etched Si surface. There, Au^{3+} ions can be reduced to Au^0 in electroless fashion to produce nanoscale Au lines (Figure 11 A).[15] Buriak and co-workers have used DPN to draw Au and Pd wires on Ge(100) surfaces based on a similar electroless surface reduction process.[16] They also generated nanopatterns on Si by applying a bias while using DPN to deliver alkynes to a H–passivated Si wafer (Figure 11 C,D).[66] Electrically driven DPN processes have even been used to pattern biomolecules onto surfaces. Stone and co-workers have demonstrated high-resolution patterning of several different proteins on nickel using this method (Figure 11 B).[67]

Sols can be patterned by direct-write DPN, which allows the generation of solid-state dielectric and magnetic nanostructures.[17,18] For applications which do not require the chemical complexity afforded by DNA-directed orthogonal assembly, or where the final target is a fluorescent material[10,68] or conducting polymer,[8–10] such approaches can provide a direct route to complex nanostructures with potentially useful magnetic or optical properties.

A variety of DPN-based methods for the generation of templates that can direct the assembly of functional nanostructures have been developed. It is anticipated that the next generation of experiments will focus on using DPN as a rapid prototyping tool to fabricate arrays of nanostructures with interesting and potentially useful optical or electrical properties. At the same time, others will continue to pioneer DPN-related techniques that will make the pattern-generation process even more routine, especially at very high resolutions (< 20 nm).

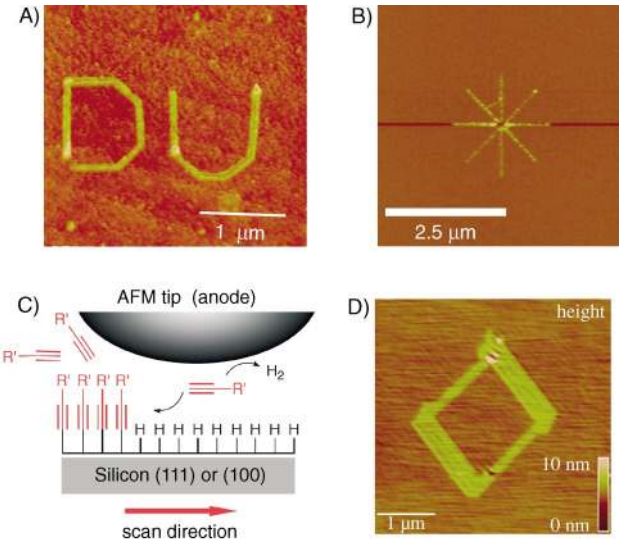

Figure 11. Electroless and electrical DPN techniques. A) $HAuCl_4$ was deposited from the DPN tip and plated by electroless deposition onto a silicon surface (reproduced with permission from ref. [15]). B) TIPA-8 protein filaments deposited on nickel under −2 V bias (reproduced with permission from ref. [67]). C) Scheme and D) results of nanopatterning by delivering alkynes to a hydrogen-passivated surface using DPN while applying an electrical bias (reproduced with permission from ref. [66]).

2.4. DPN-Patterned Etch Resists

Several methods, including electron-beam lithography,[69] photolithography,[69] micro-contact printing,[70,71] nanoimprint lithography,[72] ion-beam lithography,[73,74] and some forms of scanning-probe lithography[75] can be used to pattern inorganic materials. However, very few of these techniques offer the ability to work routinely in the sub-50-nm regime with control over feature size and interfeature distance, especially when such features are made of both hard and soft materials. Furthermore, the vast majority of these techniques, require elaborate and expensive instrumentation and are inherently single-ink processes. In this section we describe how the combination of DPN with wet chemical etching,[76] can be used to fabricate both metal and semiconductor nanostructures without requiring any hardware other than an AFM with closed-loop scanning.

DPN-generated MHA or ODT SAMs can be used as resists for creating three-dimensional (3D) multilayered solid-state structures by standard wet-etching techniques (Figure 12). A scanning electron microscopy (SEM) image of a portion of a 40000-dot array (Figure 12 A) shows the

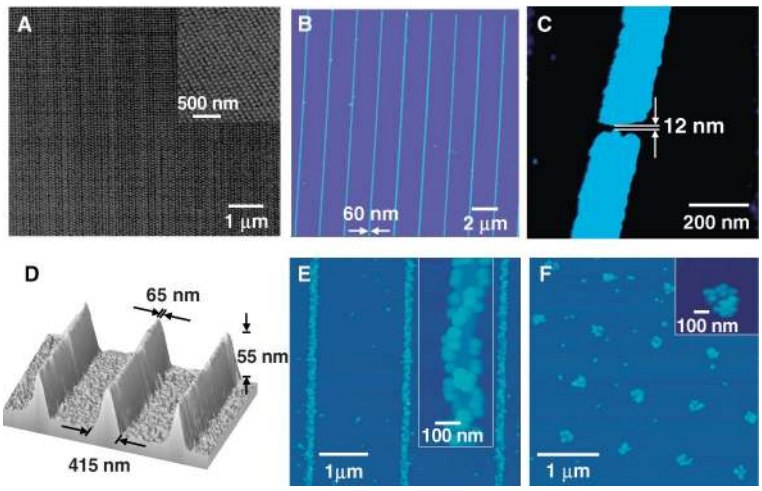

Figure 12. Etched nanostructures. A) SEM image of 45-nm gold nanodots (reproduced with permission from ref. [6]), B) TM-AFM image of 60-nm gold nanolines (reproduced with permission from ref. [77]) and C) 12-nm gold nanogap (reproduced with permission from ref. [6]) on a Si/SiO_x surface. D) 3D Si(100) nanostructures[4]). TM-AFM image of DNA-modified line (E), and dot (F), features after hybridization with complementary DNA-modified nanoparticles; insert: high-resolution TM-AFM images.[5]

regularity of the feature size and interfeature distance. The actual dot diameter as measured by SEM is approximately 45 nm. The uniformity of the nanostructures is quite good, which demonstrates the ability to fabricate high quality sub-50-nm features using the DPN process. At present, the smallest-diameter dot structures that have been made with this method are 25 ± 5 nm.[6] By using this method, we have been able to generate complex features including lines, circles, triangles, and dots. Figure 12B shows a typical etched gold nanoline array with line widths of 60 nm.[77] Importantly, because DPN can be used to deliberately make almost any sort of feature regardless of shape and size (up to the many-micrometer length scale), the technique also can be used to generate nanoelectrode gaps in the range of 12 to 100 nm (Figure 12C).[6] The ability to generate gold features also provides a route to generate structured semiconductor surfaces. By using the gold of the etched features as a resist, nanoscale patterns can be etched into an underlying silicon substrate. By removing the residual gold with aqua regia, nanofeatures composed of silicon can thus be produced (Figure 12D).[4]

Gold surface features can be treated with other inorganic (e.g., gold nanoparticles) and/or biological materials (e.g., DNA, proteins, viruses, peptides) to form hybrid bioinorganic nanoarrays. After etching, the nanostructures are still coated with MHA or ODT, and it is difficult to conduct subsequent gold-thiol modifications on the features that make up the array. However, by irradiating the array with a UV lamp and subsequently rinsing it with Milli-Q H_2O, the oxidized monolayer of MHA can be removed[78–80] to generate gold nanostructures that are easily modified with other thiol-containing molecules. As one example, it was shown that the freshly prepared gold nanopatterns can be functionalized with a disulfide-functionalized oligonucleotide.[5] To demonstrate that the oligonucleotides were, in fact, adsorbed onto the gold patterns and not on the other areas of the array, their hybridization properties were studied with 30-nm gold particles functionalized with complementary DNA by a three-strand system.[5] TM-AFM images of the arrays show that the particles hybridize to the oligonucleotide-functionalized gold nanofeatures but not the areas surrounding these features (Figure 12E and F).[5] High-resolution images of the dots and lines clearly show the individual particles on the nanofeatures.

DPN-generated etch resists provide a straightforward way of creating arrays of inorganic nanostructures (e.g., Au, Ag, Pd) on a semiconducting or an insulating surface. The ease of use and accessibility of AFM systems (as compared to electron-beam lithography/SEM systems for instance) are major advantages of the DPN-based approach to hard-nanostructure fabrication. Furthermore, the resulting structures can be selectively modified with adsorbates that provide additional and desirable functionality. By combining these etching approaches with direct-write deposition of molecular and biomolecular inks described above, it will be possible to generate an even wider variety of functional nanostructures.

3. Ink Transport: Experiment and Theory

Developing an understanding of the tip–substrate ink transport process not only is a fundamental issue, but also is important to the further development of DPN as a workhorse nanofabrication technique. A better understanding of ink-transport processes would facilitate efforts to develop more rapidly and optimize new ink–substrate combinations, help efforts to improve the resolution of DPN (which is presently in the 15-nm range under optimum conditions),[2] and guide efforts to fabricate custom tips, integrated inking systems and parallel cantilever arrays for high-throughput patterning (see Section 4).

Tip–substrate molecular transport is a complicated process and likely to be influenced by numerous parameters. These include the chemical makeup (and purity) of both the ink and surface, the tip shape, composition, and surface chemistry, the distribution and mobility of ink on the tip, and the temperature under which the experiment is carried out. Furthermore, except under UHV conditions, some form of full or partial water adlayer will be present on the patterning surface. Under ambient conditions, a water meniscus can condense between the tip and the surface. Under most conditions then, it seems apparent that the presence of ambient moisture will influence the DPN process, just as it affects the imaging resolution of contact-mode AFM in air. Given these facts, the humidity at which the patterning is carried out, and the water solubility of the ink will influence the DPN deposition process. Because of the influence of humidity on the transport of various inks, it is prudent to encase AFM instruments used for DPN in a humidity-

Figure 13. An AFM (Park Scientific AutoProbe CP Research) encased in a humidity-controlled glove box (PlasLabs) for temperature- and humidity-controlled DPN experiments.

controlled glove box (Figure 13) or environmental chamber. This system provides a controllable and reproducible environment for performing DPN experiments, and allows a user to switch samples and conduct multiple experiments with the same environmental parameters.

Over the past year, several experiments have quantified the effects of humidity and temperature on the DPN patterning of various inks. De Yoreo and co-workers studied the deposition of MHA on gold substrates as a function of contact time and humidity.[22] They observed faster deposition at higher humidities and interpreted their results as a combination of the kinetics of ink dissolution into the meniscus and of the size of the meniscus. On the other hand, Sheehan and Whitman conducted a similar study on ODT and found only a negligible dependence of the writing speed on the ambient humidity.[23] In parallel with these groups, we conducted a systematic study of the DPN deposition of both MHA and ODT as a function of varying humidity and temperature.[33] Consistent with the results of both De Yoreo and Sheehan and Whitman, MHA was found to exhibit an increase in deposition rate at elevated humidity, while ODT showed little if any dependence. As noted above, however, molecular transport from the AFM tip to the surface depends on many variables, and our results showed that the magnitude of the humidity dependence could depend on the temperature at which the experiment was carried out (and vice versa).[33] Such results underscore the need for careful control over experimental conditions to facilitate valid comparisons between studies being conducted in the multiparameter space of a typical DPN experiment (and certainly help account for some of the variability in the early data). The differences in behavior between ODT and MHA can be explained in terms of their different solubilities in the water meniscus. This interpretation is consistent with the temperature dependence of the deposition rates as well as their humidity dependence. Such an interpretation is also supported by our data which showed that the deposition of DNA oligomers (one of the most hydrophilic inks studied to date) was extremely sensitive to the ambient humidity (with faster deposition occurring at higher humidities, and no observable transport at low humidity ($<30\,\%$)).[12]

One surprising result from these initial experiments has been that for the DPN deposition of molecules ranging from simple alkanethiols[33] to oligonucleotides,[12] and from silazanes[81] to conducting polymers,[9] the growth of feature size with contact time exhibits an extremely similar functional form (although the "rate constants" for each molecular class can vary widely). For the patterning of dots (by holding the AFM tip in stationary contact with the surface) this functional form was first fit as a linear dependence of dot area, a, with contact time, t (square-root dependence of dot diameter with contact time) [Eq. (1)] with k serving as a (ink, temperature,

$$a = k\,t + b \tag{1}$$

humidity, etc. dependent) fitting parameter, and b corresponding to a tip size/coating dependent parameter.

This fit is consistent with the AFM tip serving as a source of constant ink flux, and has been modeled by Schatz, Ratner, and co-workers in terms of two-dimensional (2D) diffusion with a source.[82] More recently, Sheehan and Whitman have challenged the assumption of a constant ink flux from the AFM tip, and have suggested that the tip be modeled as a source of constant ink concentration.[23] Their results yield an expression for the surface ink concentration as a function of both deposition time and distance from the AFM tip. Their calculations appear to match their data slightly better than those with Equation (1) over the range of contact times studied. However, to date, neither model has been tested systematically over a large range (several orders of magnitude) of contact times. Such an experiment would serve to differentiate more clearly between the assumptions of the tip serving as a source of constant flux and constant concentration. It is possible that under different conditions (type of molecule, scan speed, temperature, humidity, etc.) the tip may be more accurately modeled by one assumption over the other. In this regard, it is worth noting that De Yoreo and coworkers were able to fit their data in terms of Equation (1),[22] but with two different rate constants at different times. These two rates were attributed to the regimes in which the kinetics of ink detachment from the tip (at short contact times/high scan speeds) and ink diffusion (at long contact times/slow scan speeds), respectively, limit the growth kinetics. Underscoring the importance of molecular properties, some types of molecules can also exhibit "anomalous" diffusion properties in DPN experiments and produce fractal-like rather than circular features (Figure 14).[21]

It seems natural that the effects of temperature and humidity will vary depending on the nature of the molecules

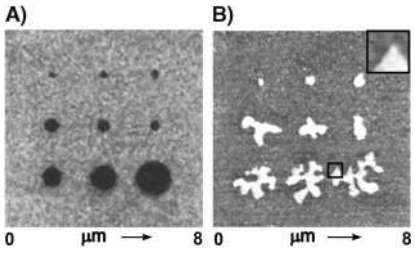

Figure 14. "Normal" diffusion (A) observed for ODT on gold, and "anomalous" diffusion (B) observed for 1-dodecylamine on mica, inset: higher-resolution image. Reproduced with permission from ref. [21].

used, and this is indeed consistent with most experience. It is even possible that different molecules are transported to the surface by fundamentally different mechanisms. Comparing the transport properties of an aliphatic thiol, such as ODT with those of DNA provides a particularly vivid demonstration of these issues. Several groups have demonstrated that the deposition rate of ODT is only slightly affected by humidity. In contrast, it was found that with oligonucleotide inks, the area of spots generated at constant contact times could be varied by nearly an order of magnitude by a change in relative humidity of less than 20 percent. DNA is difficult to pattern at either very low humidities (where no deposition was observed) or very high humidities (where the rapid flow of DNA from the cantilever to the surface prevented the generation of nanoscale patterns). For different molecules, it is possible that similar phenomena could arise from effects ranging from variations in the viscosity of hygroscopic ink solutions as they equilibrate with the ambient environment, to the size of the water meniscus formed between the tip and the surface.

On the theoretical side, Schatz, Ratner, and Jang recently studied the condensation of a liquid meniscus between an AFM tip and a surface using a grand canonical Monte Carlo simulation of a 2D lattice gas.[83] They included a variety of effects in their model (such as the wettability and curvature of the AFM tip) that should be important to the DPN process. These studies provide important insights, and make qualitative predictions on the dependence of DPN feature sizes on ambient humidity—at least under the assumption that deposition is under thermodynamic control and related to the size of the meniscus.

Although these studies provide a promising start, much work remains to be done (in terms of both experiment and theory). On the theory side, it is likely that a complete simulation of the DPN process will require models which combine the thermodynamics of meniscus formation with the dynamic effects of ink desorption, transport through the meniscus, and self-assembly. On the experimental side, more direct comparisons of transport properties for a wider range of inks under a wider range of carefully controlled conditions are needed.

Because the patterns that are deposited during DPN can be imaged in situ using AFM/LFM as they are formed, DPN itself provides a unique opportunity to study the dynamics of the monolayer nucleation and growth process. Although scanning-probe methods have been applied previously to obtain molecular-resolution images of SAM structure, formation, and growth,[84–86] DPN brings a new level of experimental control to such studies. In particular, the serial nature of such an experiment allows the monolayer growth to be modulated in both a *site*-specific and time-controlled fashion, which facilitates a step-by-step imaging of the surface modification process, and side-by-side comparisons of a continuous gradient of conditions on a single surface. In conjunction with Hong, we first applied this approach to the study of ODT and MHA monolayer formation.[87] Rather than holding the AFM tip in a single location to form dots, coated tips were raster-scanned rapidly across a substrate while acquiring a series of images (note that a complete theory of DPN deposition will ultimately need to explain deposition in this rapid-scan mode as well as dot formation at long dwell times). Under ambient conditions of 30% relative humidity, it was observed that the formation of an ODT monolayer followed a nucleation and growth process, with small crystalline domains of ODT appearing at even low surface coverages. In contrast, MHA monolayers exhibited quite different growth kinetics, and were observed to coat gold terraces uniformly until saturation coverage was reached. Again, these differences were interpreted in terms of the presence of the water meniscus and the relative hydrophilicities of the ink molecules. It would be particularly informative to conduct similar studies on a systematic series of adsorbates.

In another application, we have applied DPN as a tool for the in situ study of monolayer exchange processes—another area of fundamental scientific interest as well as industrial importance.[7] DPN-initiated site-selective exchange can potentially be used to produce a variety of complex nanostructures, and is important to understand, especially in terms of the deposition of mixed monolayers, (as have been used in the controlled adsorption of virus particles discussed in Section 2.2). To study the relative rates of exchange, a series of adsorbates, including ODT, MHA, ferrocene (11-mercaptoundecyl), and ferrocene (11-mercapto-1-oxoundecyl), were patterned by DPN into a series of identical "nanolibraries" (Figure 15 A and B). This arrangement facilitates the side-by-side comparison of the exchange properties of a series of adsorbates under identical conditions as a function of feature size and composition. Furthermore, the site-selective and serial nature of the DPN initiated exchange experiment provides a way to extract kinetic data on a large number of

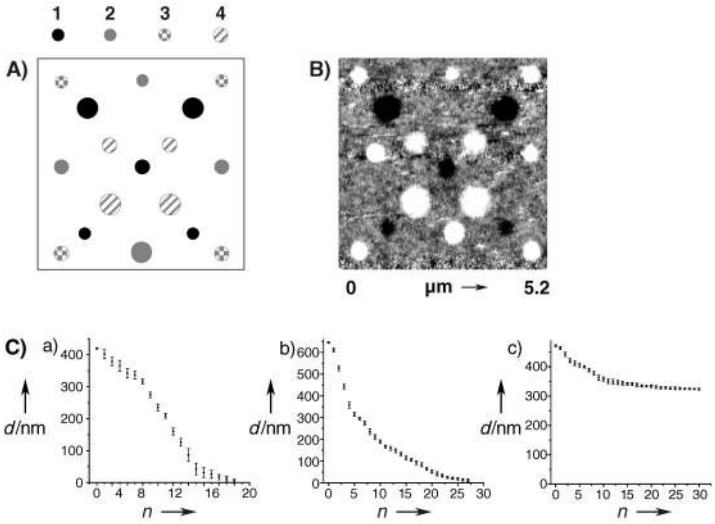

Figure 15. Studying site-selective monolayer exchange using DPN. A) Schematic representation of a combinatorial library design containing the four different molecular inks. B) LFM image of the library described in (A), collected with a clean tip at 4 Hz and contact force of 0.5 nN (24 °C, 40% relative humidity). C) Plot of dot diameter *d* as a function of number of scans *n* at 3 Hz with an ODT coated tip for a) **3**, b) **4**, and c) **2**. The library studied is in (B). **1** ODT, **2** MHA, **3** ferrocene (11-mercapto-1-oxoundecyl), **4** ferrocene (11-mercaptoundecyl). In all cases, the scan size was 5.4×5.4 μm. Reproduced with permission from ref. [7].

nearly identical nanostructures (Figure 15C). Using this method, the relative stabilities of monolayers formed from the adsorbates were deduced to be, in order of decreasing stability: MHA, ODT, ferrocene (11-mercaptoundecyl), and ferrocene (11-mercapto-1-oxoundecyl). Furthermore it was observed that the nanostructures exchanged preferentially from the outside inward, consistent with the electrochemical whittling experiments[50] described in Section 2.2, and providing evidence for a defect-mediated exchange process. This hypothesis was confirmed by experiments conducted on single-crystal gold surfaces which showed that monolayers were dramatically more stable to DPN-initiated exchange on single-crystal surfaces than on polycrystalline gold surfaces.

These experiments have only scratched the surface of what could prove to be a rich series of DPN-based ink transport, surface kinetics, and exchange studies. For instance, DPN can be used to pattern monolayer-thick diffusion barriers (corrals) on surfaces, and then selectively deposit inks within such a structure.[3] Understanding the patterns that are formed as a result requires an understanding not only of the thermodynamics of meniscus formation in the vicinity of such structures, but also the kinetics of ink diffusion across native and modified surfaces, as well as of the stability and time evolution of the surface chemistry under conditions where monolayer exchange can occur.

4. Development of High-Throughput Parallel Dip-Pen Nanolithography

Up to this point the focus of this Review has been on the progress and technology of "single-pen" DPN, which can serve as a powerful tool by enabling researchers to fabricate and study structures which would be difficult, if not impossible, to create and study with other techniques. However, like all scanning-probe-based imaging and lithographic systems, DPN is inherently a serial process. To increase the throughput and area accessible to scanning-probe techniques, several groups are pursing the development of parallel-probe cantilever arrays. In collaboration with us,[3] C. Liu and co-workers have developed MEMs-based parallel-probe strategies designed specifically with the constraints of DPN applications in mind.[92,94,95]

Among the best known parallel probe research is that conducted at IBM,[88,89] and also at Stanford University.[90,91] The primary aim of the IBM group has been in the area of high-density data storage. Towards this end they have implemented an independently addressable 32×32 probe array as part of IBM's "millipede" project. The 1024-cantilever array measures approximately 3 mm per side, and each cantilever is assigned to read and write its own approximately 100×100 μm area. The data-storage medium itself is actually a very thin film of polymer. To write a bit of data, a tip is heated to over 400 °C allowing it to sink into the polymer. Reading of data is accomplished by operating the tips at slightly lower temperatures. Those tips that fall into contact with a written bit of data are cooled more rapidly than those resting on the polymer surface. In addition, Quate and co-workers at Stanford have developed a number of 1D and 2D probe arrays for both imaging and lithographic applications. With regard to lithographic applications, their principle approach to patterning has been current-induced lithography, and they have thus developed schemes for regulating the current emitted from the tip by regulating the tip–substrate bias.[90,91]

The requirements of thermal data-transfer and current-induced lithographic methods distinguish themselves from the requirements of DPN-based applications. Because patterning in a DPN experiment occurs whenever a coated tip is held in contact with a surface, independent control of the on/off state of each cantilever in an array requires independent actuation of the force applied to, and height of, the cantilever on/above the surface—an engineering challenge that is distinct from controlling the temperature or bias applied to a cantilever. Furthermore, the goal of making parallel-probe DPN systems wide-spread and easily accessible makes fabrication costs and integration with standard AFM systems important design considerations.

The simplest implementation of parallel-pen DPN is thus a passive probe array. In this case, the pens are not actuated independently but are simultaneously brought into contact with the surface and scanned together, which allows the duplication of a single pattern a number of times equal to the number of probes in the array. The first experiments in this area used commercially available cantilevers with an inter-tip spacing of 1.4 mm.[3] Recently, the group of C. Liu has produced cantilever arrays composed of up to 10000 pens (Figure 16A). In conjunction with C. Liu and co-workers we have demonstrated writing with arrays of 32 parallel probes; images of eight 60-nm features that were written in parallel are shown in Figure 16B.[92] Since active feedback is applied to only a single cantilever in the array, and the others are allowed to track the topography passively, specific constraints on the registration between the array and the surface, as well as the flexibility of the cantilevers must be met.[92] A commercial entity, NanoInk, has begun producing prototype passive arrays with as many as a million pens (Figure 16C and D).[93] For patterning large areas in high-throughput DPN applications without sacrificing the registration capabilities of DPN, along with C. Liu, we have developed DPN tips made of polydimethylsiloxane (PDMS), we call this technique scanning-probe contact printing (SP-CP).[94]

Independent control of each probe tip is the next step, and can be accomplished using piezoelectric, capacitive, or thermoelectric actuation. In the first generation of active parallel-probe DPN arrays, thermoelectric actuation has been used: resistive heating of a multilayer cantilever results in differential expansion of the components, which leads to bending of the probe. Using this approach, a range of complex patterns can be generated at high speed because the contact between each tip and the writing surface is independently controlled. C. Liu and co-workers have also developed strategies capable of independently verifying the "on/off" state of each probe in a highly parallel array based on electrical conduction.[95]

The final challenge of complete MEMs integration of DPN technology is the automation of tip coating and ink delivery. It is proposed that custom microfluidic systems will

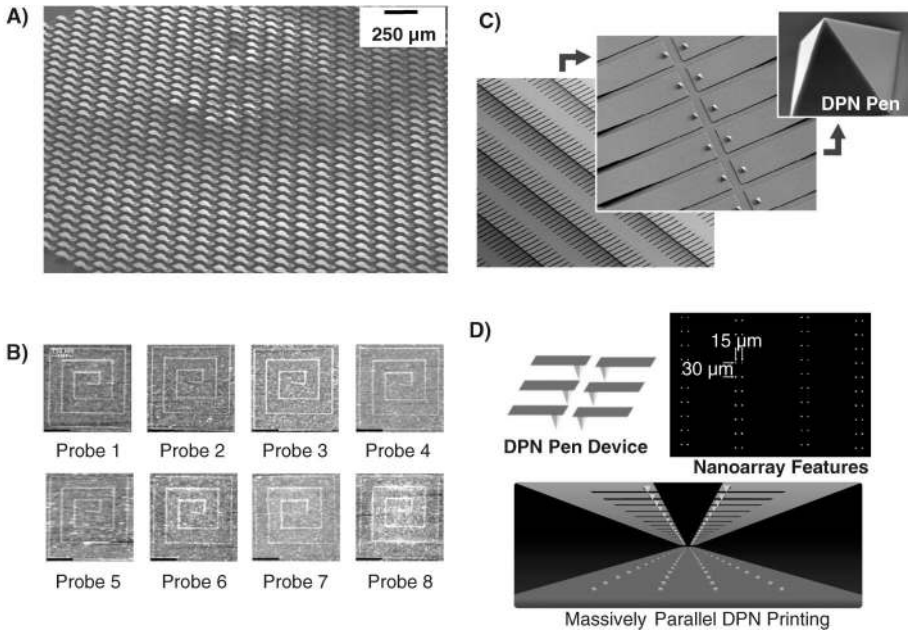

Figure 16. Parallel-probe DPN. A) SEM image of a high-density, 2D array of passive DPN probes (courtesy of Chang Liu UIUC) B) Contact-mode AFM topographic images of eight copies of ODT patterns generated by using a parallel probe array of AFM cantilevers (reproduced with permission from ref. [92]). C) SEM images of a commercial "Massively Parallel Pen" (MPP) array (courtesy of NanoInk, Inc). D) Fluorescence micrograph of spots written with the MPP array (courtesy of NanoInk, Inc.).

ultimately be used to control the inking of individual cantilevers in a parallel probe array. The realization of such systems will depend on the development and adaptation of a number of technologies. Large-scale integration of microfluidic technologies is still challenging, and arrays of 1000 individually addressable wells represent the current state-of-the-art.[96] Thus, to meet the inking needs of parallel probe arrays (with an ultimate goal of being able to deliver a different ink to each probe in a 10000-pen array), new microfluidic arrays of addressable ink wells must be implemented. Such systems are already under development.[97] In addition to microfluidic ink wells into which tips can be "dipped," integrating the microfluidics directly into the tips themselves offers another attractive possibility for MEMs engineers interested in DPN. In an extension of the DPN technique that some have likened to a "fountain pen",[98] both micro- and nanopipettes have been used as scanning-probe tips with hollow cores through which inks ranging from chemical etchants[98] to photoresist[99] and even biomolecules,[26,100] can be pumped directly to a surface for site-specific lithography. Although nanopipette-DPN work is presently restricted by the hand-fabrication of pulled glass capillaries, Espinosa and co-workers are lifting this limitation by using advances in microfabrication technology to generate massively parallel fountain-pen arrays.[101] In this regard, it is striking to note how the evolution of DPN—from a quill pen to a fountain pen to a multiple-pen plotter—has emulated the blueprint provided by the evolution of modern macro-scale writing and printing technologies. Indeed, this evolution has followed very closely the path proposed at the initial invention of DPN.[60,102–107]

5. Summary and Outlook

DPN is a unique scanning-probe-based lithographic tool for generating high-resolution patterns of chemical functionality on a range of surfaces. The combination of resolution, registration, and direct-write capability offered by DPN distinguishes it from any alternative lithographic strategy and makes DPN a promising tool for patterning soft organic and biological nanostructures. Many other recent lithographic tools that have been developed, such as microcontact patterning (μCP) and nanoimprint lithography (NIL), have been driven by the desire to create tools that can compete with existing techniques in the semiconductor arena on the basis of cost and, in the case of NIL, by offering higher resolution. An attractive feature of DPN is that it is both a tool for scientific discovery as well as an engineering advance that allows useful multicomponent nanostructures to be printed at a resolution that is superior to any conventional lithographic tool. In an age of nanotechnology, where being able to fabricate nanostructures of a certain composition, size, and shape is essential, DPN in its current state of development is already a tool that will allow for rapid advances in the science and technology of highly miniaturized structures. If the efforts to transform it into a massively parallel process are successful, it will become a powerful production tool in both the life sciences and the semiconductor industry.

This Review has covered several areas of current DPN research, including the generation of biomolecular nanoarrays for diagnostic applications as well as fundamental studies of ligand–receptor interactions. Other particularly attractive areas of DPN research include the generation of templates for assembling (and also for directly depositing) colloidal particles, as well as the creation of a variety of hard nanostructures through direct deposition as well as etching. While much remains to be learned about the DPN deposition process, particularly in the area of tip-substrate ink transport and diffusion, several studies published over the past year have begun to help clarify things. The transport of two molecules as similar as ODT and MHA can exhibit different sensitivities to their environmental conditions, and a complete theory of DPN deposition will need to combine the effects of meniscus formation as well as the kinetics of ink transport in a manner that can account for the specific chemistry of an individual ink. Finally, we have described the ongoing development of both passive and active parallel-pen DPN arrays. Although predicting the future is troublesome, it is nevertheless fascinating and fun to speculate on the possibil-

ities that would be opened when such highly parallel DPN systems are realized. High-throughput deposition of biomolecular arrays is one application that comes to mind. Today, scientists use robotic spotting systems (with only 4–16 parallel pins) to generate custom DNA and protein chips. Even modestly parallel DPN systems could compete with these systems in terms of throughput, thereby allowing the fabrication and screening of entire chips using AFM-based systems. One could imagine that similar parallel DPN systems could be applied to combinatorial studies of catalysis, as well as to the patterning of molecule-based electronic materials with high levels of registration. Finally, with respect to semiconductors, the ability to add and remove solid-state materials from an underlying substrate makes DPN a very attractive potential tool for lithographic mask fabrication, inspection, and repair. It is clear that DPN has a bright future in both its single- and multi-pen incarnations.

The Air Force Office of Scientific Research (AFOSR), Defense Advanced Research Projects Agency (DARPA), Army Research Office (ARO), and National Science Foundation (NSF) are all acknowledged for support. D.S.G. thanks the National Institutes of Health (NIH) and DuPont for postdoctoral fellowship support.

Received: May 22, 2003 [A608]

[1] R. D. Piner, J. Zhu, F. Xu, S. H. Hong, C. A. Mirkin, *Science* **1999**, *283*, 661.
[2] S. H. Hong, J. Zhu, C. A. Mirkin, *Science* **1999**, *286*, 523.
[3] S. H. Hong, C. A. Mirkin, *Science* **2000**, *288*, 1808.
[4] D. A. Weinberger, S. G. Hong, C. A. Mirkin, B. W. Wessels, T. B. Higgins, *Adv. Mater.* **2000**, *12*, 1600.
[5] H. Zhang, Z. Li, C. A. Mirkin, *Adv. Mater.* **2002**, *14*, 1472.
[6] H. Zhang, S.-W. Chung, C. A. Mirkin, *Nano Lett.* **2003**, *3*, 43.
[7] A. Ivanisevic, K. V. McCumber, C. A. Mirkin, *J. Am. Chem. Soc.* **2002**, *124*, 11997.
[8] B. W. Maynor, S. F. Filocamo, M. W. Grinstaff, J. Liu, *J. Am. Chem. Soc.* **2002**, *124*, 522.
[9] J. H. Lim, C. A. Mirkin, *Adv. Mater.* **2002**, *14*, 1474.
[10] A. Noy, A. E. Miller, J. E. Klare, B. L. Weeks, B. W. Woods, J. J. De Yoreo, *Nano Lett.* **2002**, *2*, 109.
[11] D. L. Wilson, R. Martin, S. Hong, M. Cronin-Golomb, C. A. Mirkin, D. L. Kaplan, *Proc. Natl. Acad. Sci. USA* **2001**, *98*, 13660.
[12] L. M. Demers, D. S. Ginger, S. J. Park, Z. Li, S. W. Chung, C. A. Mirkin, *Science* **2002**, *296*, 1836.
[13] M. Ben Ali, T. Ondarçuhu, M. Brust, C. Joachim, *Langmuir* **2002**, *18*, 872.
[14] Y. Li, B. W. Maynor, J. Liu, *J. Am. Chem. Soc.* **2001**, *123*, 2105.
[15] B. W. Maynor, Y. Li, J. Liu, *Langmuir* **2001**, *17*, 2575.
[16] L. A. Porter, H. C. Choi, J. M. Schmeltzer, A. E. Ribbe, L. C. C. Elliott, J. M. Buriak, *Nano Lett.* **2002**, *2*, 1369.
[17] L. Fu, X. G. Liu, Y. Zhang, V. P. Dravid, C. A. Mirkin, *Nano Lett.* **2003**, *3*, 757.
[18] M. Su, X. G. Liu, S. Y. Li, V. P. Dravid, C. A. Mirkin, *J. Am. Chem. Soc.* **2002**, *124*, 1560.
[19] J. Hyun, S. J. Ahn, W. K. Lee, A. Chilkoti, S. Zauscher, *Nano Lett.* **2002**, *2*, 1203.
[20] N. A. Amro, S. Xu, G.-y. Liu, *Langmuir* **2000**, *16*, 3006.
[21] P. Manandhar, J. Jang, G. C. Schatz, M. A. Ratner, S. Hong, *Phys. Rev. Lett.* **2003**, *90*, 115505.
[22] B. L. Weeks, A. Noy, A. E. Miller, J. J. De Yoreo, *Phys. Rev. Lett.* **2002**, *88*, 255505.
[23] P. E. Sheehan, L. J. Whitman, *Phys. Rev. Lett.* **2002**, *88*, 156104.
[24] G. Agarwal, L. A. Sowards, R. R. Naik, M. O. Stone, *J. Am. Chem. Soc.* **2003**, *125*, 580.
[25] R. McKendry, W. T. S. Huck, B. Weeks, M. Florini, C. Abell, T. Rayment, *Nano Lett.* **2002**, *2*, 713.
[26] A. Bruckbauer, L. M. Ying, A. M. Rothery, D. J. Zhou, A. I. Shevchuk, C. Abell, Y. E. Korchev, D. Klenerman, *J. Am. Chem. Soc.* **2002**, *124*, 8810.
[27] S. Matsubara, H. Yamamoto, K. Oshima, E. Mouri, H. Matsuoka, *Chem. Lett.* **2002**, 886.
[28] Y. M. Jung, S. J. Ahn, E. R. Kim, H. Lee, *J. Korean Phys. Soc.* **2002**, *40*, 712.
[29] X. Hong, L. Wei, W. Guo, J. Li, W. L. Song, Y. B. Bai, T. J. Li, *Chem. J. Chin. Univ.* **2002**, *23*, 1778.
[30] L. Wei, X. Hong, W. Guo, Y. B. Bai, T. J. Li, *Chem. J. Chin. Univ.* **2002**, *23*, 1386.
[31] J. H. Liao, L. Huang, N. Gu, *Chin. Phys. Lett.* **2002**, *19*, 134.
[32] H. L. Zhang, Y. Guo, H. L. Li, D. Q. Yang, *Chem. J. Chin. Univ.* **1999**, *20*, 1460.
[33] S. Rozhok, R. Piner, C. A. Mirkin, *J. Phys. Chem. B* **2003**, *107*, 751.
[34] K. B. Lee, S. J. Park, C. A. Mirkin, J. C. Smith, M. Mrksich, *Science* **2002**, *295*, 1702.
[35] S. P. A. Fodor, *Science* **1997**, *277*, 393.
[36] E. S. Lander, *Nat. Genet.* **1999**, *21*, 3.
[37] D. R. Walt, *Science* **2000**, *287*, 451.
[38] A. Schulze, J. Downward, *Nat. Cell Biol.* **2001**, *3*, E190.
[39] M. Kato-Maeda, Q. Gao, P. M. Small, *Cell. Microbiol.* **2001**, *3*, 713.
[40] P. G. Marciano, J. H. Eberwine, R. Raghupathi, T. K. McIntosh, *Restor. Neurol. Neurosci.* **2001**, *18*, 105.
[41] F. F. Bier, F. Kleinjung, *Fresenius J. Anal. Chem.* **2001**, *371*, 151.
[42] D. S. Wilson, S. Nock, *Angew. Chem.* **2003**, *115*, 510; *Angew. Chem. Int. Ed.* **2003**, *42*, 494.
[43] R. C. Jin, Y. W. Cao, C. A. Mirkin, K. L. Kelly, G. C. Schatz, J. G. Zheng, *Science* **2001**, *294*, 1901.
[44] R. Elghanian, J. J. Storhoff, R. C. Mucic, R. L. Letsinger, C. A. Mirkin, *Science* **1997**, *277*, 1078.
[45] T. A. Taton, C. A. Mirkin, R. L. Letsinger, *Science* **2000**, *289*, 1757.
[46] J. H. Lim, D. S. Ginger, K. B. Lee, J. Heo, J. M. Nam, C. A. Mirkin, *Angew. Chem.* **2003**, *115*, 2411; *Angew. Chem. Int. Ed.* **2003**, *42*, 2309.
[47] K. B. Lee, J. H. Lim, C. A. Mirkin, *J. Am. Chem. Soc.* **2003**, *125*, 5588.
[48] H. J. Dai, N. Franklin, J. Han, *Appl. Phys. Lett.* **1998**, *73*, 1508.
[49] G.-Y. Liu, N. A. Amro, *Proc. Natl. Acad. Sci. USA* **2002**, *99*, 5165.
[50] Y. Zhang, K. Salaita, J. H. Lim, C. A. Mirkin, *Nano Lett.* **2002**, *2*, 1389.
[51] M. Mrksich, *Curr. Opin. Chem. Biol.* **2002**, *6*, 794.
[52] J. C. Smith, K.-B. Lee, Q. Wang, M. G. Finn, J. E. Johnson, M. Mrksich, C. A. Mirkin, *Nano Lett.* **2003**, *3*, 883.
[53] C. L. Cheung, J. A. Camarero, B. W. Woods, T. W. Lin, J. E. Johnson, J. J. De Yoreo, *J. Am. Chem. Soc.* **2003**, *125*, 6848.
[54] Q. Wang, T. W. Lin, J. E. Johnson, M. G. Finn, *Chem. Biol.* **2002**, *9*, 813.
[55] Q. Wang, E. Kaltgrad, T. W. Lin, J. E. Johnson, M. G. Finn, *Chem. Biol.* **2002**, *9*, 805.
[56] L. M. Demers, C. A. Mirkin, *Angew. Chem.* **2001**, *113*, 3159; *Angew. Chem. Int. Ed.* **2001**, *40*, 3069.
[57] J. P. Hoogenboom, D. L. J. Vossen, C. Faivre-Moskalenko, M. Dogterom, A. van Blaaderen, *Appl. Phys. Lett.* **2002**, *80*, 4828.
[58] J. Aizenberg, P. V. Braun, P. Wiltzius, *Phys. Rev. Lett.* **2000**, *84*, 2997.

[59] A. Ivanisevic, J. H. Im, K. B. Lee, S. J. Park, L. M. Demers, K. J. Watson, C. A. Mirkin, *J. Am. Chem. Soc.* **2001**, *123*, 12424.
[60] C. A. Mirkin, *MRS Bull.* **2000**, *25*, 43.
[61] N. C. Seeman, A. M. Belcher, *Proc. Natl. Acad. Sci. USA* **2002**, *99*, 6451.
[62] C. M. Niemeyer, *Angew. Chem.* **2001**, *113*, 4254; *Angew. Chem. Int. Ed.* **2001**, *40*, 4128.
[63] A. P. Alivisatos, K. P. Johnsson, X. G. Peng, T. E. Wilson, C. J. Loweth, M. P. Bruchez, P. G. Schultz, *Nature* **1996**, *382*, 609.
[64] L. M. Demers, S. J. Park, T. A. Taton, Z. Li, C. A. Mirkin, *Angew. Chem.* **2001**, *113*, 3161; *Angew. Chem. Int. Ed.* **2001**, *40*, 3071.
[65] J. C. Garno, Y. Y. Yang, N. A. Amro, S. Cruchon-Dupeyrat, S. W. Chen, G.-Y. Liu, *Nano Lett.* **2003**, *3*, 389.
[66] P. T. Hurley, A. E. Ribbe, J. M. Buriak, *J. Am. Chem. Soc.* **2003**, *125*, 11334.
[67] G. Agarwal, R. R. Naik, M. O. Stone, *J. Am. Chem. Soc.* **2003**, *125*, 7408.
[68] M. Su, V. P. Dravid, *Appl. Phys. Lett.* **2002**, *80*, 4434.
[69] G. M. Wallraff, W. D. Hinsberg, *Chem. Rev.* **1999**, *99*, 1801.
[70] Y. N. Xia, J. A. Rogers, K. E. Paul, G. M. Whitesides, *Chem. Rev.* **1999**, *99*, 1823.
[71] Y. Xia, G. M. Whitesides, *Angew. Chem.* **1998**, *110*, 568; *Angew. Chem. Int. Ed.* **1998**, *37*, 550.
[72] S. Y. Chou, *MRS Bull.* **2001**, *26*, 512.
[73] M. Albrecht, C. T. Rettner, A. Moser, M. E. Best, B. D. Terris, *Appl. Phys. Lett.* **2002**, *81*, 2875.
[74] Y. S. Kim, W. Hong, H. J. Woo, H. W. Choi, G. D. Kim, J. H. Lee, S. Lee, *Jpn. J. Appl. Phys. Part 1* **2002**, *41*, 4141.
[75] G. Y. Liu, S. Xu, Y. L. Qian, *Acc. Chem. Res.* **2000**, *33*, 457.
[76] Y. N. Xia, X. M. Zhao, E. Kim, G. M. Whitesides, *Chem. Mater.* **1995**, *7*, 2332.
[77] H. Zhang, K.-B. Lee, Z. Li, C. A. Mirkin, *Nanotechnology* **2003**, *14*, 1113.
[78] M. J. Tarlov, D. R. F. Burgess, G. Gillen, *J. Am. Chem. Soc.* **1993**, *115*, 5305.
[79] J. Y. Huang, J. C. Hemminger, *J. Am. Chem. Soc.* **1993**, *115*, 3342.
[80] J. Y. Huang, D. A. Dahlgren, J. C. Hemminger, *Langmuir* **1994**, *10*, 626.
[81] A. Ivanisevic, C. A. Mirkin, *J. Am. Chem. Soc.* **2001**, *123*, 7887.
[82] J. K. Jang, S. H. Hong, G. C. Schatz, M. A. Ratner, *J. Chem. Phys.* **2001**, *115*, 2721.
[83] J. K. Jang, G. C. Schatz, M. A. Ratner, *J. Chem. Phys.* **2002**, *116*, 3875.
[84] G. E. Poirier, E. D. Pylant, *Science* **1996**, *272*, 1145.
[85] G. E. Poirier, M. J. Tarlov, *Langmuir* **1994**, *10*, 2853.
[86] C. A. Widrig, C. A. Alves, M. D. Porter, *J. Am. Chem. Soc.* **1991**, *113*, 2805.
[87] S. H. Hong, J. Zhu, C. A. Mirkin, *Langmuir* **1999**, *15*, 7897.
[88] P. Vettiger, M. Despont, U. Drechsler, U. Durig, W. Haberle, M. I. Lutwyche, H. E. Rothuizen, R. Stutz, R. Widmer, G. K. Binnig, *IBM J. Res. Dev.* **2000**, *44*, 323.
[89] W. P. King, T. W. Kenny, K. E. Goodson, G. L. W. Cross, M. Despont, U. T. Durig, H. Rothuizen, G. Binnig, P. Vettiger, *J. Microelectromech. Syst.* **2002**, *11*, 765.
[90] E. M. Chow, G. G. Yaralioglu, C. F. Quate, T. W. Kenny, *Appl. Phys. Lett.* **2002**, *80*, 664.
[91] T. Sulchek, R. J. Grow, G. G. Yaralioglu, S. C. Minne, C. F. Quate, S. R. Manalis, A. Kiraz, A. Aydine, A. Atalar, *Appl. Phys. Lett.* **2001**, *78*, 1787.
[92] M. Zhang, D. Bullen, S. W. Chung, S. Hong, K. S. Ryu, Z. F. Fan, C. A. Mirkin, C. Liu, *Nanotechnology* **2002**, *13*, 212.
[93] L. M. Demers, G. della Cioppa, *Genet. Eng. News* **2003**, *23*, 32.
[94] X. Wang, K. S. Ryu, D. A. Bullen, J. Zou, H. Zhang, C. A. Mirkin, C. Liu, *Langmuir* **2003**, *19*, 8951.
[95] J. Zou, D. Bullen, X. F. Wang, C. Liu, C. A. Mirkin, *Appl. Phys. Lett.* **2003**, *83*, 581.
[96] T. Thorsen, S. J. Maerkl, S. R. Quake, *Science* **2002**, *298*, 580.
[97] D. Banerjee, J. Fragala, T. Duenas, R. Shile, B. Rosner in *Proceedings of the Seventh International Symposium on Miniaturized Chemical and Biochemical Analysis (micro-TAS 2003)* (Squaw Valley, October 5–9, 2003), **2003**, *1*, 58.
[98] A. Lewis, Y. Kheifetz, E. Shambrodt, A. Radko, E. Khatchatryan, C. Sukenik, *Appl. Phys. Lett.* **1999**, *75*, 2689.
[99] M. H. Hong, K. H. Kim, J. Bae, W. Jhe, *Appl. Phys. Lett.* **2000**, *77*, 2604.
[100] A. Bruckbauer, D. J. Zhou, L. M. Ying, Y. E. Korchev, C. Abell, D. Klenerman, *J. Am. Chem. Soc.* **2003**, *125*, 9834.
[101] K.-H. Kim, C. Ke, N. Moldovan, H. D. Espinosa in *Proceedings of the Society of Experimental Mechanics Annual Conference* (Charlotte, NC, 2.–4. June 2003), **2003**, 235.
[102] C. A. Mirkin, *Inorg. Chem.* **2000**, *39*, 2258.
[103] C. A. Mirkin, R. D. Piner, S. Hong, U.S. Patent App. No. 20020063212, May 24, **2001**.
[104] C. A. Mirkin, S. Hong, V. P. Dravid, U.S. Patent App. No. 20020122873, Jan. 28, **2002**.
[105] C. A. Mirkin, G. della Cioppa, L. Demers, K.-B. Lee, S.-J. Park, U.S. Patent App. No. 20030068446, Oct. 2, **2002**.
[106] C. A. Mirkin, V. P. Dravid, M. Su, X. Liu, U.S. Patent App. No. 20030162004, Dec. 17, **2002**.
[107] C. A. Mirkin, R. Piner, S. Hong, U.S. Patent App. No. 20030157254, Nov. 22, **2002**.
[108] X. G. Liu, S. W. Liu, C. A. Mirkin, *Angew. Chem.* **2003**, *115*, 4785; *Angew. Chem. Int. Ed.* **2003**, *42*, 4933.
[109] H. Jung, R. Kulkarni, C. P. Collier, *J. Am. Chem. Soc.* **2003**, *125*, 12096.
[110] X. G. Liu, L. Fu, S. H. Hong, V. P. Dravid, C. A. Mirkin, *Adv. Mater.* **2002**, *14*, 231.
[111] D. J. Pena, M. P. Raphael, J. M. Byers, *Langmuir* **2003**, *19*, 9028.
[112] M. Su, S. Y. Li, V. P. Dravid, *J. Am. Chem. Soc.* **2003**, *125*, 9930.

